HHS Public Access

Author manuscript

Cancer. Author manuscript; available in PMC 2020 March 01.

Published in final edited form as:

Cancer. 2019 March 01; 125(5): 807–817. doi:10.1002/cncr.31851.

A Clinical Trial of Intraoperative Near Infrared Imaging to Assess Tumor Extent and Identify Residual Disease During Anterior Mediastinal Tumor Resection

Jarrod D. Predina, MD, MTR[1,2], **Jane Keating, MD**[1], **Andrew Newton, MD**[1,2], **Christopher Corbett, BA**[1,2], **Leilei Xia, MBBS**[1,2], **Michael Shin, BA**[1,2], **Lydia Frenzel Sulfyok, BA**[1,2], **Charuhas Deshpande, MD**[3], **Leslie Litzky, MD**[3], **Shuming Nie, PhD**[4], **John C. Kucharczuk, MD**[1,2], and **Sunil Singhal, MD**[1,2,*]

[1]Center for Precision Surgery, Perelman School of Medicine at the University of Pennsylvania

[2]Department of Surgery, Perelman School of Medicine at the University of Pennsylvania

[3]Department of Pathology, Perelman School of Medicine at the University of Pennsylvania

[4]Department of Chemistry, University of Illinois

Abstract

Introduction: Management of most solid tumors of the anterior mediastinum involves complete resection. Given location near mediastinal structures, wide resection is not possible; therefore, surgeons must utilize subjective visual and tactile cues to determine disease extent. In this clinical trial we explore intraoperative near-infrared (NIR) imaging as an approach to improve tumor delineation during mediastinal tumor resection.

Methods: Twenty-five subjects with anterior mediastinal lesions suspicious for malignancy were enrolled in an open-label, feasibility trial. Subjects received indocyanine-green (5mg/kg) 24 hours prior to resection (a technique called TumorGlow). NIR imaging systems included the Artemis (Quest, Netherlands) and the Iridium (VisionSense, USA). Intratumoral indocyanine-green uptake was evaluated. Clinical value was determined by assessing the ability of NIR imaging to detect phrenic nerve involvement or incomplete resection. Clinical and histopathologic variables were analyzed to determine predictors of tumor fluorescence.

Results: No drug-related toxicity was observed. Optical imaging added a mean of 11 minutes to case duration. Among subjects with solid tumors, 19 of 20 accumulated indocyanine-green. Fluorescent tumors included thymomas (n=13), thymic carcinomas (n=4), and liposarcomas (n=2). NIR feedback improved phrenic nerve dissection (n=4) and identified residual disease (n=2). There were no false-positives or false-negatives. Indocyanine-green preferentially accumulated in solid tumors; this was independent of clinical and pathologic variables.

*Corresponding Author. 6 White building; 3400 Spruce St. Philadelphia, PA 19104. Sunil.singhal@uphs.upenn.edu. Ph: 215-662-4767. Fax: 215-615-6562.

Author Contributions: JDP and SS contributed to project conception, patient enrollment, data acquisition, data analysis and manuscript preparation. JK, AN, CC, LX, MS, LFS contributed to data acquisition, data analysis and manuscript preparation. CD, LL, SN, JCK contributed to patient enrollment, data acquisition, data analysis and manuscript preparation.

Conflicts of Interest: None

Conclusions: NIR imaging for anterior mediastinal neoplasms is safe and feasible. This technology may provide a real-time tool capable of determining tumor extent, and specifically identify phrenic nerve involvement and residual disease.

Precis:

During resection of anterior mediastinal masses, intraoperative identification of phrenic nerve involvement and positive margins may be challenging. Near-infrared imaging may provide a real-time tool capable of determining tumor extent, and specifically identify phrenic nerve involvement and residual disease.

Keywords

anterior mediastinum; thymoma; surgery; intraoperative imaging; optical imaging; ICG

Introduction:

Primary tumors of the anterior mediastinum encompass a diverse group of neoplasms [1]. Despite histologic heterogeneity, standard-of-care treatment is largely similar for most solid neoplasms and requires complete surgical resection and adjuvant therapy [2–6]. Complete resection is the most important prognostic factor predicting improved survival [2–6]. In order to achieve complete resection, surgeons visually evaluate and palpate tissues to determine disease extent. Unfortunately, visual and tactile cues are subjective, somewhat dependent on experience, and may therefore lead to erroneous decisions resulting in local recurrences or unnecessary sacrifice of important structures, such as the phrenic nerve.

Near-infrared (NIR) optical imaging has recently been proposed as an intraoperative tool capable of distinguishing tumors, confirming margins and identifying positive lymph nodes from surrounding normal tissues [7–11]. Intraoperative NIR imaging requires intravenous delivery of tumor-targeted optical contrast agents that collect within tumor aggregates. One approach involves systemic delivery of the NIR contrast agent, indocyanine-green (ICG), with NIR imaging occurring 24 hours later (an approach called TumorGlow). ICG is an appealing optical agent given its excellent safety profile and its propensity to accumulate in a diverse array of tumor histologies via the enhanced permeability and retention (EPR) [12, 13]. EPR permits nanostructures (between 10nm and 100nm) to accumulate in solid malignancies as a result of leaky vasculature and the lack of lymphatics [14].

Our group has initially explored this approach in clinical trials involving patients with pulmonary metastases [12] and non-small cell lung cancer (NSCLC) [13]. In these feasibility studies, NIR imaging was capable of identifying both subcentimeter malignant lesions and positive margins. More recently, we applied this approach to preclinical models of anterior mediastinal neoplasms, and observed excellent sensitivity following neoadjuvant chemotherapy [15]. These preclinical successes have thus set the stage for clinical translation of intraoperative NIR imaging for resectable anterior mediastinal tumors.

In this report, we explore NIR intraoperative imaging in 25 patients who underwent resection for suspicious anterior mediastinal tumors. More specifically, we primarily sought

to evaluate safety and feasibility of NIR imaging with ICG in patients with anterior mediastinal neoplasms. As a clinical endpoint, secondary goals were to determine if the fluorescent signature could provide reliable real-time intraoperative information that could improve identification of phrenic nerve involvement or incomplete resection.

Materials and Methods:

Study Drug:

Patients were infused with a 5mg/kg dose of indocyanine green (ICG) (Akorn Pharmaceuticals, Decatur, Illinois; $C_{43}H_{47}N_2O_6S_2$ Na, molecular weight 774.9 kDa) 24 hours prior to resection as previously described by our group, TumorGlow® [9, 16]. ICG is a near-infrared contrast agent with an excitation wavelength of 805nm and an emission wavelength of 830nm. ICG is a well-tolerated optical contrast agent, approved by the US Food and Drug Administration (FDA), and has been used for several decades as an imaging agent for vasculature and lymphatics.

Imaging Device:

In situ, real-time fluorescent imaging was performed using two systems optimized for detection of ICG: The Artemis (Quest, Netherlands) and the Iridium (VisionSense Corp, Philadelphia, PA) as previously described [9, 16, 17]. The Artemis imaging systems was utilized for Subjects 1–10, while the Iridium was used for Subjects 11–25. Both devices are high definition, dual band (white light and NIR) camera systems capable of concurrent NIR emission and detection while generating real-time video. The Artemis system incorporates an excitation laser with peak intensity of 793nm and selects NIR signal using a long-pass filter set to 808nm. The Iridium system utilizes an excitation laser with a wavelength of 805nm, with fluorescence detection based on a bandpass filter selective to light ranging from 825 to 850nm. During VATS and robotic procedures, systems were equipped with NIR-calibrated thoracoscopes. For *ex vivo* evaluation, the thoracoscopes were removed and an exoscope was used.

Study Design:

This non-randomized, open-label, single-arm, single-center feasibility trial (NCT02651246) was approved by the University of Pennsylvania Institutional Review Board. All subjects provided informed consent and were recruited between December 2015 and November 2017. In total, 25 subjects were enrolled. The primary goal of this study was to evaluate safety and feasibility of NIR imaging with ICG in patients with anterior mediastinal neoplasms. Secondary objectives included confirming ICG accumulation within mediastinal tumors and determining if fluorescent signature could impact phrenic nerve management.

Twenty-five provided informed consent and were enrolled. Sample size and study design were based on consensus guidelines provided by the World Molecular Imaging Society [18]. All subjects presented with anterior mediastinal neoplasms identified by preoperative high-resolution CT scanning. Although several patients presented with a preoperative tissue diagnosis, this was not an inclusion criterion. For imaging studies obtained outside the University of Pennsylvania Health System (UPHS), at least one UPHS thoracic radiologist

reviewed preoperative imaging to confirm the presence of an anterior mediastinal mass, rule-out metastatic disease, and confirm findings of preoperative imaging.

All subjects were scheduled for a resection via median sternotomy, transcervical, VATS, or robotic resection. Surgical approach was based surgeon preference, which incorporated clinical, pathologic, and anatomic variables. Twenty-four hours prior to resection, all subjects received intravenous ICG (5mg/kg) in the University of Pennsylvania Health System's Clinical Translational Research Center [9, 16]. Patients were monitored for 1 hour and then discharged. Of note, dosing parameters were determined based on preclinical data involving thymoma models [15] and previous human data involving other pleural based and intrapulmonary neoplasms [12, 13, 19].

The following day patients return for tumor resection. During surgery, surgeons utilized standard visualization and finger palpation (when applicable) to identify known tumors. After identification of the tumor, NIR imaging was used to confirm lesion fluorescence. If the preoperatively identified nodule was unidentifiable by white-light visualization or palpation, localization using fluorescence guidance was attempted. After identifying the mediastinal mass, fluorescence imaging was utilized to assess tumor involvement of mediastinal structures (phrenic nerve, aorta, pleura, etc.) and then to confirm complete resection. All lesions were resected when possible and imaged *ex vivo* prior to submitting for histopathologic examination by a pulmonary pathologist.

Safety was assessed by periodic subject evaluation from infusion to postoperative follow-up (2–4 weeks following resection). Routine laboratory studies were obtained at post-operative day one or if indicated. Adverse events were described using Common Terminology Criteria for Adverse Events (CTCAE), Version 4.03 [20].

Histopathologic and Fluorescent Microscopic Review of Specimens:

Excised specimens were formalin fixed and paraffin embedded. Sequential 5μm sections were obtained and underwent comprehensive histopathologic and fluorescent analysis by a board-certified thoracic pathologist. Sections were stained using standard hematoxylin/eosin (H&E) staining. Immunohistochemical (IHC) staining for CD31, a marker of endothelial cells, was performed. To understand ICG accumulation patterns at a microscopic level, an additional unstained 5μm section was evaluated using a NIR microscopic scanner (*Odyssey*, LiCor, Lincoln, NE). Areas of fluorescence were then correlated to both H&E and anti-CD31 IHC specimens.

Statistical Analysis:

Post hoc image analysis was performed to quantify the amount of fluorescence using region of interest (ROI) software within ImageJ (free software program available through the National Institute of Health; http://rsb.info.nih.gov/ij). A background fluorescence level was also obtained, and tumor-to-background fluorescence ratio (TBR) was calculated for all identified lesions. Data are presented as mean (standard deviation) unless otherwise noted. Differences between groups were assessed by a student's t-test or an ANOVA test. Given the exploratory nature of this study, multiple predictions models were made to assess patient and histopathologic variables that were predict *in situ* tumor fluorescence. All comparisons were

made use Stata Statistical Software: Release 14 (College Station, TX: StataCorp LP). A p-value of 0.05 or less was considered statistically significant.

Results:

Patients Data:

Between December 2015 and November 2017, 25 subjects (n=15 male) with a mean age of 58 years (SD, 16 years) met inclusion criteria and successfully underwent anterior mediastinal tumor resection with NIR imaging. The mean tumor size by preoperative CT was 5.7cm (range1.1–19.5cm). Final pathologic evaluation of tumors revealed thymoma (n=13), thymic carcinoma (n=4), lymphoma/hematologic malignancy (n=3), liposarcoma (n=2), ectopic thyroid (n=2), and teratoma (n=1). Subjects most commonly underwent resection via partial/median/thoraco-sternotomy (n=13), robotic resection (n=6), transcervical resection (n=5), and traditional VATS resection (n=1). Three patients received neoadjuvant chemotherapy for a diagnosis of thymic carcinoma. Table 1 provides a complete summary of subject and histopathologic data characteristics.

Safety and Feasibility Data:

All subjects received the complete dose of intravenous ICG on average 23.9 hours (SD, 3.8 hours) prior to resection. Intraoperative imaging added a median of 11 minutes (range, 5 minutes to 15 minutes) to the case duration. No drug related adverse events were encountered during drug infusion, intraoperatively or postoperatively after 30 days of follow-up.

Anterior Mediastinal Solid Tumors Accumulate ICG and Display NIR Fluorescence:

During resection, 21 of 25 (92%) lesions displayed fluorescence upon NIR imaging (Figure 1a–d). Fluorescent lesions included thymoma (n=13), thymic carcinoma (n=4), liposarcoma (n=2), and hematologic malignancies (n=2). Histopathologic evaluation of non-fluorescent lesions revealed benign ectopic thyroid (n=2), a B-cell Lymphoma (n=1), and a mature teratoma (n=1).

Upon subgroup analysis, 19 of 20 solid tumors displayed tumor-specific fluorescence patterns. For the 19 solid malignancies displaying NIR signal, the mean tumor-associated fluorescence intensity was 117.2 AU (SD, 38.4 AU), which was significantly higher than benign thymus and surrounding mediastinal fat (background) which measured 28.5 AU (SD, 14.8 AU); $p<0.001$ (Figure 2a–c). Based on these values, the mean TBR of fluorescent tumors was 5.2 (SD, 3.1) (Figure 2f). Of note, 2 of 2 benign lesions (ectopic thyroid) were non-fluorescent, while 2 of 3 hematologic neoplasms displayed fluorescence.

To confirm selective intratumoral ICG accumulation at a microscopic level, all resected specimens were analyzed using by brightfield techniques and NIR microscopic scanning. In each of the fluorescent tumors, dye accumulation was found to be primarily within tumors, rather than in surrounding benign tissues including thymic fat, pleura and lung parenchyma (Figure 3a, 3b). By additional immunohistochemical analyses, we found tumors to be highly vascular with expression of the endothelial marker, CD31 (Figure 3c, 3d)

Post-Resection Wound Bed Inspection with NIR Imaging Confirms Complete Resection of Macroscopic Disease:

Following resection among the 20 subjects with solid tumors, NIR inspection of the post-operative wound bed was suggestive of complete resection in 18 subjects (Figure 4a). Results were confirmed by frozen section and by final pathologic assessment for each patient, thus conveying a 100% negative predictive value.

Of the 13 subjects undergoing resection for thymoma; 4 subjects were found to have Masaoka Stage I disease, 5 were found to have Masaoka Stage IIa disease, and 4 were found to have Masaoka Stage IIb disease. There were no patients with Masaoka Stage III or IV disease.

Wound Bed Inspection with NIR Mapping Identifies Incomplete Resection:

In 2 of 20 patients, fluorescent evaluation revealed suspicious areas concerning for residual tumor. (Figure 4b, 4c). Both Subjects 4 and 14 presented for resection of thymic carcinomas and were status-post neoadjuvant chemotherapy. Following initial resection, areas of patchy fluorescence measuring greater than 2cm were identified along the aortic groove, pericardium and visceral pleural surface. Upon frozen analysis, tumor involvement was confirmed at the resection margin. Given aortic involvement, no additional resection was performed. There were no false negatives after pathologic review the margins of resected specimens.

Real-time Fluorescent Information Improves Assessment of Phrenic Nerve Involvement:

Mediastinal tumor resection is dictated by anatomic boundaries which include unresectable organs; however, the phrenic nerve is a structure which may be sacrificed if necessary. Because phrenic nerve management is based primarily on visual and tactile information available to the surgeon, we were interested the addition of NIR imaging could impact this therapeutic challenge.

Four of 20 (20%) subjects were found to have mediastinal tumors within close proximity to the phrenic nerve upon gross inspection (representative example provided Figure 5a). Among these 4 tumors (Subjects 4, 7, 13, 19), histology included thymic carcinoma (n=2), thymoma (n=1), and liposarcoma (n=1). In general, these tumors were large (mean 11.2cm, range 7.1–19.5cm) and were approached via sternotomy. By white-light visualization and finger palpations, surgeons found difficulty in confirming a lack of phrenic nerve involvement (Figure 5b). By contrast, gross evaluation with the addition of NIR optical feedback allowed for rapid determination of nerve involvement, given a mean tumor-to-phrenic nerve fluorescence ratio of 2.7 (Figure 5c). In each case, tumor specific signal generated reliable feedback which enhanced safe dissection from the tumor (Figure 5d). Fluorescent feedback suggested complete resection with no residual disease adherent to the phrenic nerve in each case (Figure 5e). NIR information was confirmed with clear tumor margins being noted by both frozen-section and final pathologic review for each patient.

Pathologic and clinical variables predicting fluorescence of NIR imaging:

in situ intraoperative fluorescence is critical for maximum benefit of this approach. Given the exploratory nature of this study, the relation of TBR to several clinical and pathologic variables was assessed: lesion type (solid tumor vs hematologic malignancy/benign disease), tumor size, subject age, subject gender, tumor histology and time to NIR imaging (Figure 6). We found that only lesion type predicted TBR, with solid tumors displaying significantly higher TBRs as compared to hematologic malignancies or benign lesions (Figure 6a). The mean TBR of solid tumors was noted to be 5.3 versus 1.9 in other lesions; p=0.03. Trends favoring increased *in situ* TBR were associated with larger tumors (p=0.14) and older age (p=0.15); however, did not reach statistical significance. Other examined variables did not predict tumor fluorescence.

Discussion:

Complete resection of anterior mediastinal neoplasms is critical and can be challenging given a location adjacent to vital structures. In this report, we explore NIR intraoperative imaging with ICG as an intraoperative adjunct that may improve tumor identification and resection accuracy. We found that 95% of solid anterior mediastinal neoplasms accumulate ICG and demonstrate real-time fluorescence upon NIR imaging. In a select cohort of patients, optical information may assist the surgeon when assessing for phrenic nerve involvement and may confirm complete tumor resection. This report details the only successful trial of NIR imaging for anterior mediastinal neoplasms and is the first to demonstrate a potential clinical role of NIR imaging during oncologic resection. This approach appears applicable across a variety of surgical approaches.

ICG is a water-soluble molecule that exhibits excitation and emission in the NIR range (λ_{ex} 805 and λ_{em} 830nm, respectively) [9, 16]. ICG has commonly been used in the clinic as a tool to evaluate perfusion by NIR angiography [21, 22]. As a perfusion agent, ICG is delivered at a dose of 0.2–0.4mg/kg with fluorescent imaging occurring in the “first window” after intravenous infusion (within 10–20 minutes) [16, 21, 22]. More recently, our group has evaluated ICG as a tumor mapping probe with imaging occurring in the “second window”. This approach, also called TumorGlow, requires delivery of ICG at a higher dose (5mg/kg) with imaging occurring approximately 24 hours following drug delivery. When implementing these delivery parameters, ICG functions by exploiting abnormally leaky capillaries and increased pressure gradients (also known as the EPR effect) which are found in most solid malignancies [14]. This approach has been successful in the context of central nervous system tumors [16], pulmonary metastases [12], and primary lung neoplasms [13].

In this trial, we found ICG-based NIR imaging safe, with no patients experiencing drug-related toxicity. The low toxicity further authenticates the safety profile we observed in experiences with “second window ICG” for neurologic malignancies and thoracic malignancies [12, 13, 16]. In terms of feasibility, we found that this approach minimally impacts standard preoperative and operating room care. To elaborate, subjects received ICG on the day prior to their scheduled operation in an on-campus drug infusion center. Following drug delivery, patients were observed for approximately 30–60 minutes to rule out immediate toxicity. On the following day, subjects presented to the preoperative area as per

routine and underwent assessment while completing preoperative checklists. During resection, real-time images were displayed high-resolution operating room monitors, which added fewer than 10 minutes to case duration. Overall, surgeons found the approach efficient and high-throughput.

During NIR imaging, we found solid tumors accumulate dye more avidly than hematologic malignancies and benign disease. Nineteen of 20 solid tumors displayed robust signal upon *in vivo* fluorescent imaging. Signal was present in a variety of tumors, and after neoadjuvant chemotherapy delivery in 3 subjects with thymic carcinomas. Unlike our previous experiences in which NIR imaging with ICG was highly sensitive, these data reveal a high-degree of tumor specificity in the scenario anterior mediastinal neoplasms. On further subgroup analysis, these patterns seem independent of tested patient and pathologic variables and may suggest broad applicability to solid tumors located in the anterior mediastinum. Mechanistically, intratumoral accumulation appears to be driven by the presence of abnormal endothelial cells and high vascularity of these lesions, suggesting a role of EPR as has been described by our group [12, 13, 19].

From a clinical perspective, fluorescence provided a reliable tool to which helped surgeons perform two intraoperative tasks: (1) assessing phrenic nerve involvement and (2) evaluating the surgical wound bed for residual disease. In 4 of 20 patients, we found real-time NIR imaging influential in phrenic nerve preservation, and feel that this approach may be most useful for large tumors that are suspicious for phrenic nerve invasion based on preoperative imaging. In 2 additional subjects, residual disease was identified which was confirmed by pathologic evaluation. Unfortunately, in both subject the disease was unresectable, which begs to question the utility of this approach in identifying resectable disease in the wound bed. We point out that all 6 events were noted in patients with fairly large tumors who underwent resection via sternotomy.

We do acknowledge several limitations to this approach. First, based on the obtained data one is unable to assess the sensitivity of optical imaging with ICG for detection of microscopic residual disease. In this study cohort we were successful in identifying complete resection in all but 2 subjects. In those two subjects, we identified only macroscopic residual disease. Furthermore, in the 13 subjects presenting with thymoma, none presented with Masaoka Stage III/IV disease. There were also no occult positive margins based on pathologic review. In future studies, it will be important to characterize how this approach functions at lower thresholds of detection which is of greater clinical relevance. Next, this approach provides no information that can help identify benign thymus. This information would be particularly important for the myasthenic patient undergoing resection for thymoma. Interestingly, a recent report by Wada and colleagues have proposed several visual range dyes which can effectively target the benign thymus in preclinical models [23]. Several of these thymus-targeted agents display excitation and emission parameters within the 600–700nm range, which would allow for simultaneous imaging with ICG. Although proposed dyes have not been fully evaluated in clinical trial at this point, this approach may indeed be one that can work in concert with our proposed imaging approach.

Notwithstanding these limitations, we find intraoperative NIR imaging with ICG safe and feasible in 25 subjects presenting with resectable anterior mediastinal lesions. A high degree of tumor-specific uptake provides information that can help the surgeon rapidly and reliably assess phrenic nerve involvement and, potentially, identify residual disease. Benefits of this approach seem to be most tangible in patients presenting with large, solid tumors that are approached via sternotomy. Additional investigations will focus on optimizing dosing parameters, understanding sensitivity in detection of microscopic residual disease, and exploring this approach for localization of ectopic parathyroid adenomas.

Acknowledgments

Funding Sources: JDP was supported by a grant by the American Philosophical Society, by the NIH (F32 CA210409) and by an Association for Academic Surgery Research Grant. SS was supported by the NIH (R01 CA193556).

References:

1. Castro CY and Chhieng DC, Cytology and surgical pathology of the mediastinum. Adv Exp Med Biol, 2005 563: p. 42–54. [PubMed: 16433122]
2. Shintani Y, et al., Multimodality treatment for advanced thymic carcinoma: outcomes of induction therapy followed by surgical resection in 16 cases at a single institution. Gen Thorac Cardiovasc Surg, 2015 63(3): p. 159–63. [PubMed: 25311849]
3. Parker D, et al., Effective treatment for malignant mediastinal teratoma. Thorax, 1983 38(12): p. 897–902. [PubMed: 6198739]
4. Modh A, et al., Treatment Modalities and Outcomes in Patients With Advanced Invasive Thymoma or Thymic Carcinoma: A Retrospective Multicenter Study. Am J Clin Oncol, 2016 39(2): p. 120–5. [PubMed: 24390276]
5. Moore KH, et al., Thymoma: trends over time. Ann Thorac Surg, 2001 72(1): p. 203–7. [PubMed: 11465180]
6. Sarkaria IS, et al., Resection of primary mediastinal non-seminomatous germ cell tumors: a 28-year experience at memorial sloan-kettering cancer center. J Thorac Oncol, 2011 6(7): p. 1236–41. [PubMed: 21610519]
7. Keating JJ, Kennedy GT, and Singhal S, Identification of a subcentimeter pulmonary adenocarcinoma using intraoperative near-infrared imaging during video-assisted thoracoscopic surgery. J Thorac Cardiovasc Surg, 2015 149(3): p. e51–3. [PubMed: 25827389]
8. Okusanya OT, et al., Intraoperative molecular imaging can identify lung adenocarcinomas during pulmonary resection. J Thorac Cardiovasc Surg, 2015 150(1): p. 28–35 e1. [PubMed: 26126457]
9. Keating J, et al., Near-Infrared Intraoperative Molecular Imaging Can Locate Metastases to the Lung. Ann Thorac Surg, 2017 103(2): p. 390–398. [PubMed: 27793401]
10. Hachey KJ, et al., Safety and feasibility of near-infrared image-guided lymphatic mapping of regional lymph nodes in esophageal cancer. J Thorac Cardiovasc Surg, 2016 152(2): p. 546–54. [PubMed: 27179838]
11. Gilmore DM, et al., Identification of metastatic nodal disease in a phase 1 dose-escalation trial of intraoperative sentinel lymph node mapping in non-small cell lung cancer using near-infrared imaging. J Thorac Cardiovasc Surg, 2013 146(3): p. 562–70; discussion 569–70. [PubMed: 23790404]
12. Keating J, et al., Near-Infrared Intraoperative Molecular Imaging Can Locate Metastases to the Lung. Ann Thorac Surg, 2016.
13. Okusanya OT, et al., Intraoperative near-infrared imaging can identify pulmonary nodules. Ann Thorac Surg, 2014 98(4): p. 1223–30. [PubMed: 25106680]

14. Jiang JX, et al., Optimization of the enhanced permeability and retention effect for near-infrared imaging of solid tumors with indocyanine green. Am J Nucl Med Mol Imaging, 2015 5(4): p. 390–400. [PubMed: 26269776]
15. Keating JJ, et al., Intraoperative imaging identifies thymoma margins following neoadjuvant chemotherapy. Oncotarget, 2016 7(3): p. 3059–67. [PubMed: 26689990]
16. Lee JY, et al., Intraoperative Near-Infrared Optical Imaging Can Localize Gadolinium-Enhancing Gliomas During Surgery. Neurosurgery, 2016 79(6): p. 856–871. [PubMed: 27741220]
17. van Driel PB, et al., Characterization and evaluation of the artemis camera for fluorescence-guided cancer surgery. Mol Imaging Biol, 2015 17(3): p. 413–23. [PubMed: 25344146]
18. Tummers WS, et al., Regulatory Aspects of Optical Methods and Exogenous Targets for Cancer Detection. Cancer Res, 2017 77(9): p. 2197–2206. [PubMed: 28428283]
19. Predina JN, AD; Lee MK; Singhal S, Near-Infrared Intraoperative Imaging Can Successfully Identify of Malignant Pleural Mesothelioma after Neoadjuvant Chemotherapy Mol Imaging, 2017 16: p. 1536012117723785. [PubMed: 28856921]
20. SERVICES, U.S.D.O.H.A.H., Common Terminology Criteria for Adverse Events (CTCAE) Version 4.0. 2010.
21. Alander JT, et al., A review of indocyanine green fluorescent imaging in surgery. Int J Biomed Imaging, 2012 2012: p. 940585. [PubMed: 22577366]
22. Boni L, et al., Clinical applications of indocyanine green (ICG) enhanced fluorescence in laparoscopic surgery. Surg Endosc, 2015 29(7): p. 2046–55. [PubMed: 25303914]
23. Wada H, et al., Intraoperative Near-Infrared Fluorescence Imaging of Thymus in Preclinical Models. Ann Thorac Surg, 2017 103(4): p. 1132–1141. [PubMed: 27964920]

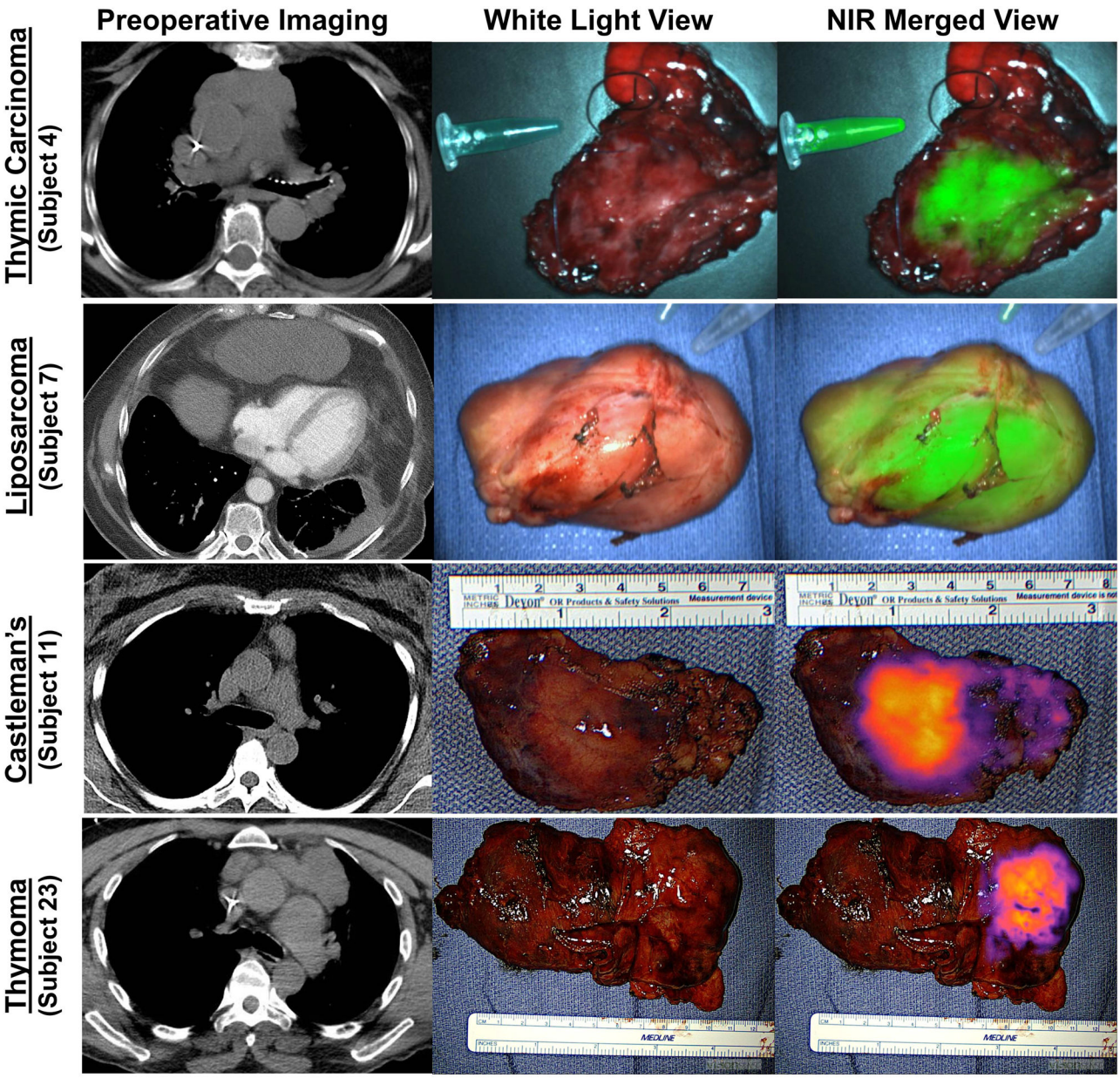

Figure 1: ICG accumulation within anterior mediastinal neoplasms generate NIR signal upon intraoperative fluorescent imaging.

Representative images of anterior mediastinal neoplasms are provided: thymic carcinoma, liposarcoma, hematologic malignancy (Castleman's Disease), and thymoma. First Column-preoperative CT; Second Column-standard white light view; Third Column-NIR merged view.

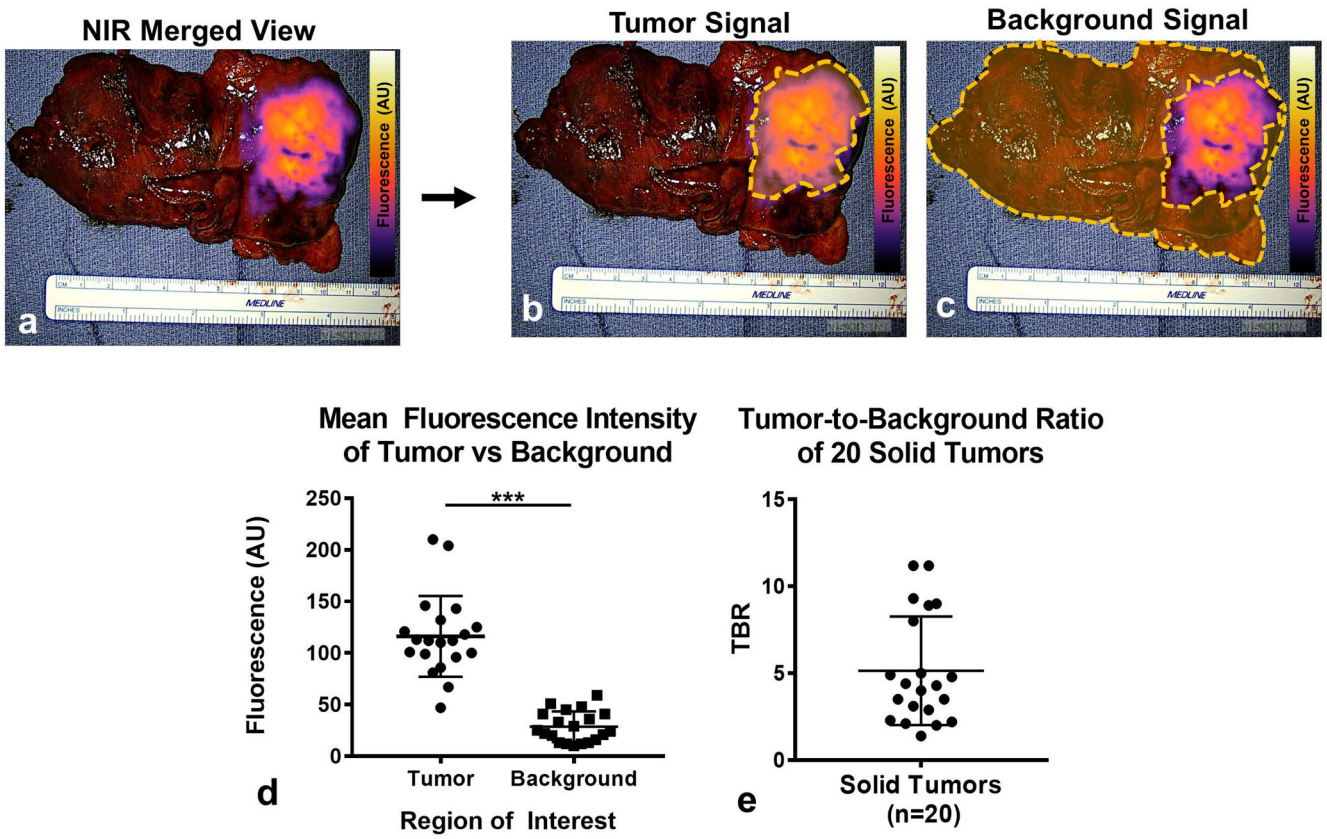

Figure 2: ICG preferentially accumulates within tumors and generates tumor-specific signal.

All specimens underwent fluorescent tomographic analysis to quantify tumor-specific fluorescence intensity. Subject 23 is provided as a representative example (**a**): NIR merged images were analyzed by quantifying the mean fluorescent intensity of (**b**) tumors and (**c**) background. (**d**) Mean fluorescent intensity of tumors were compared to background and plotted for all patients (n=20) with solid tumors. (**e**) Tumor-to-background fluorescence ratios (TBRs) were calculated and then plotted for the cohort.

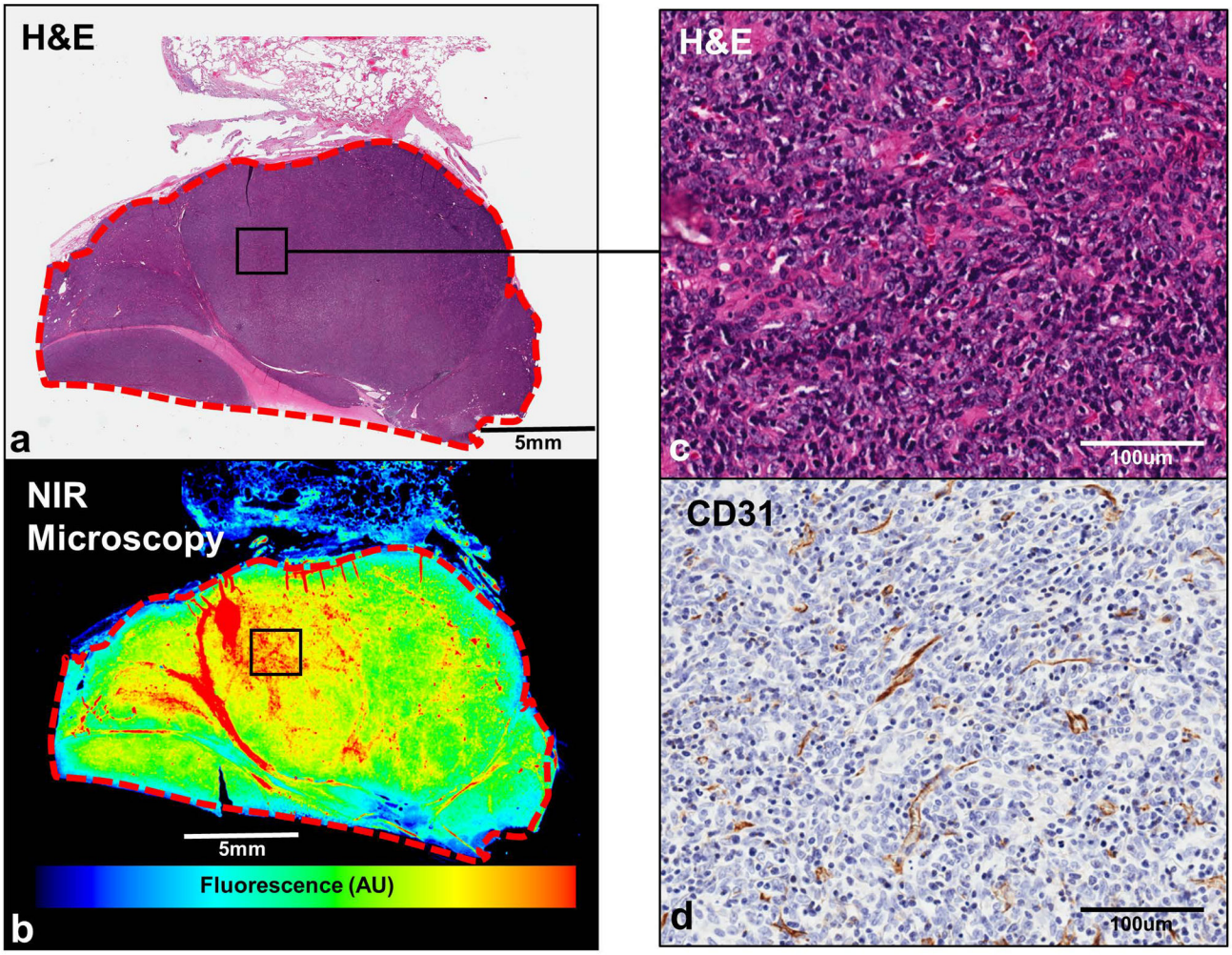

Figure 3:

Anterior Mediastinal Tumors accumulate ICG.All resected specimens underwent a series of brightfield and NIR analyses to confirm intratumoral ICG accumulation. Subject 23 (thymoma) is displayed as a representative example. As can be seen by comparing H&E (a) to NIR point scanning (b), ICG accumulation is predominantly observed within the tumor. Upon anti-CD31 IHC, we note the presence of endothelial cells within anterior mediastinal tumors (c and d).

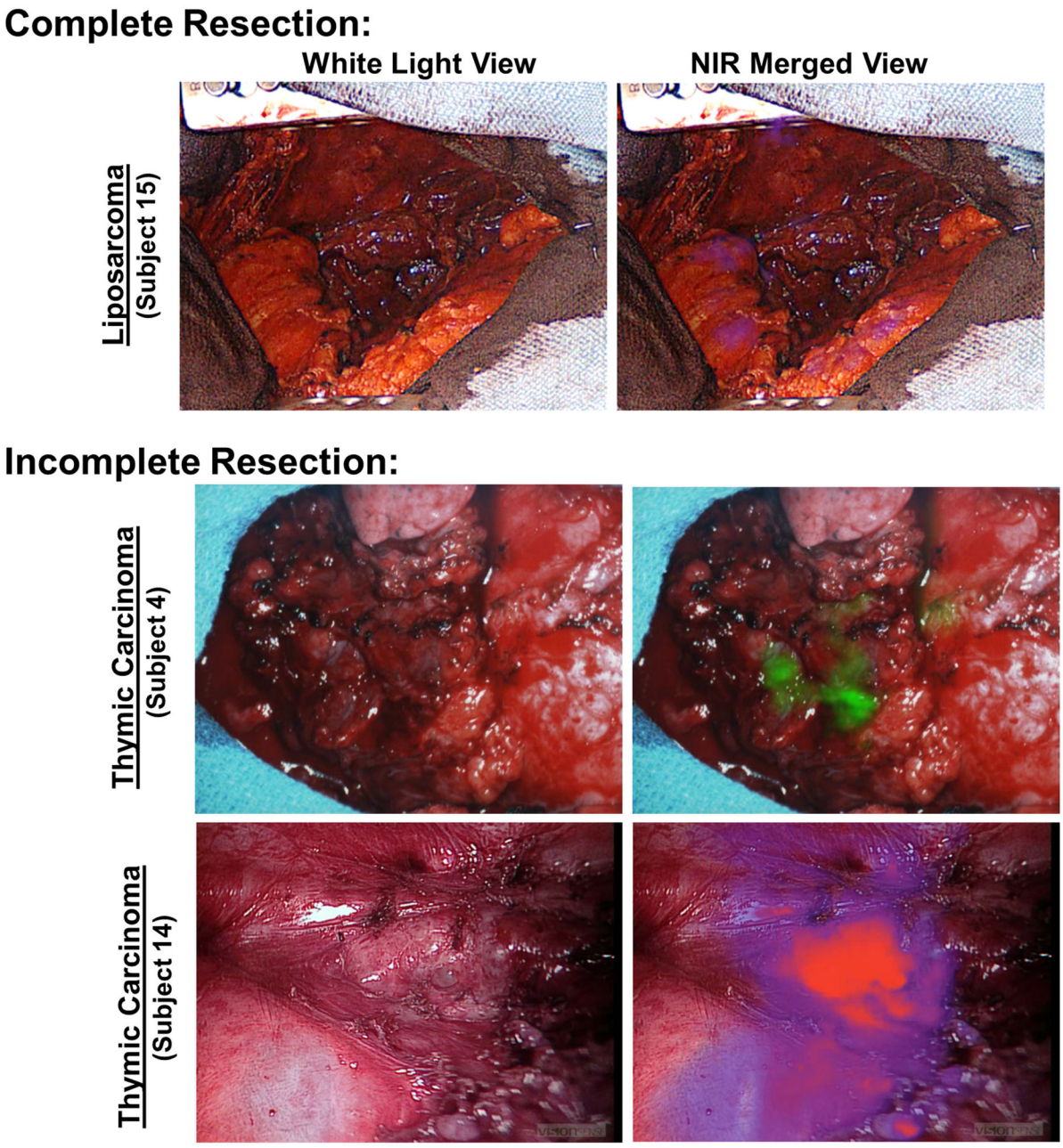

Figure 4: NIR imaging identifies unresected disease in the postoperative wound bed.

Following resection, the postoperative wound bed was inspected using NIR imaging. In 18 of 20 subjects with solid tumors, there was no evidence of residual disease (Subject 15 as representative example). In two subjects, residual macroscopic tumor deposits were identified along the aortic groove, pericardium and pleural surface (Subjects 4 and 14).

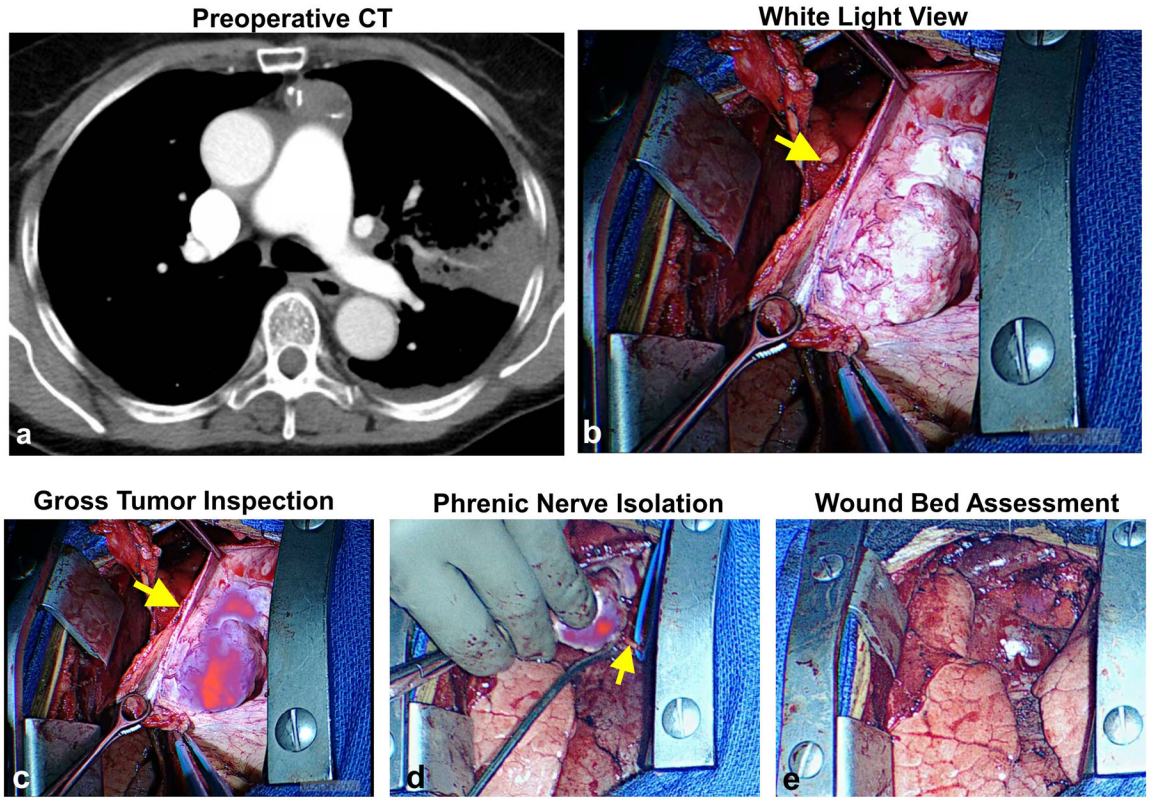

Figure 5: Fluorescent imaging provides real-time information during dissection of tumor form phrenic nerve.

In four subjects, mediastinal tumors were found in close proximity the phrenic nerve. Using fluorescent information, tumors were carefully dissected thus preserving the phrenic nerve. Data from Subject 13 is provided as a representative example. Preoperative CT (**a**) and intraoperative bright light views (**b**) of a 7.1cm thymoma. During resection, the tumor displayed high fluorescence relative to the phrenic nerve (**c**). Using real-time fluorescent information, the tumor was carefully dissected from the nerve (**d**). No residual tumor was identified after tumor resection (**e**).

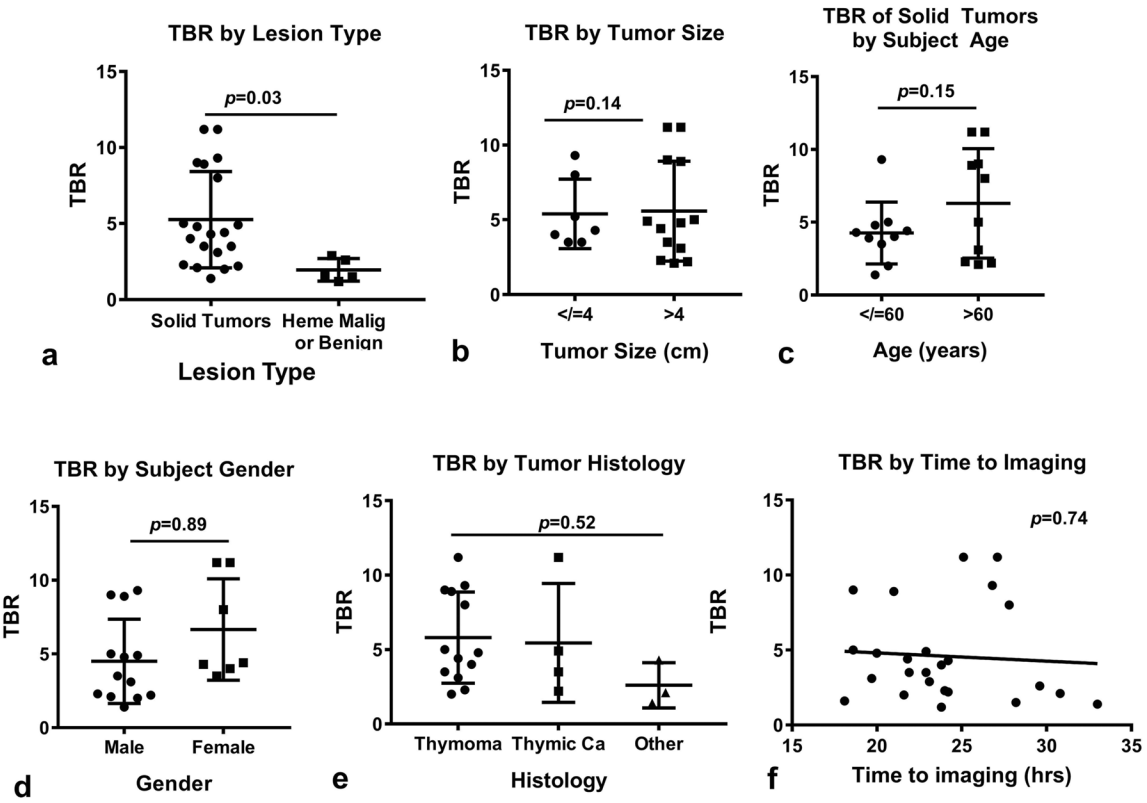

Figure 6: Clinical and histopathologic variables predicting *in situ* fluorescence:

(**a**) TBR as a function of tumor type, (**b**) TBR as a function of tumor size, (**c**) TBR as a function tumor subject age, (**d**) TBR as a function of subject gender, (**e**) TBR by tumor histology, and (**f**) TBR by time to imaging.

Table 1:

Patient and Tumor Characteristics

ID	Age (years)	Sex	Size (cm)	Time to imaging (hrs)	*In situ* TBR	Histology	Surgical Approach
1	31	F	3.1	23.8	4.0	Thymoma	R
2	65	M	7.0	24.2	2.2	Thymic Carcinoma	MS
3	25	M	5.2	33.0	1.4	Germ cell tumor/Teratoma	MS
4	76	F	8.5	25.1	11.2	Thymic Carcinoma	MS
5	60	M	3.5	21.6	2.0	Thymoma	VATS
6	57	F	2.0	29.6	2.6	Hodgkin's Lymphoma	TC
7	79	M	19.5	30.8	2.1	Liposarcoma	MS
8	53	F	6.5	21.8	4.4	Thymoma	MS
9	84	F	6.8	27.1	11.2	Thymoma	MS
10	66	M	6.5	24.0	2.3	Thymoma	R
11	45	F	2.3	23.1	2.9	Castleman's Disease	R
12	82	M	6.0	18.6	9.0	Thymoma	MS
13	77	F	7.1	22.9	3.5	Thymoma	MS
14	35	M	1.1	18.1	1.6	B-cell Lymphoma	TC
15	39	F	2.7	24.2	4.3	Liposarcoma	MS
16	60	M	12.8	18.6	5.0	Thymoma	MS
17	73	F	3.6	27.8	8.0	Thymoma	R
18	76	M	5.5	19.7	3.1	Thymoma	R
19	59	M	10.0	22.9	4.9	Thymic Carcinoma	MS *
20	48	M	1.8	28.2	1.5	Ectopic Thyroid	TC
21	53	F	1.5	23.8	1.2	Ectopic Thyroid	TC
22	60	M	3.8	26.8	9.3	Thymoma	R
23	48	M	9.1	20.0	4.8	Thymoma	MS
24	51	M	1.4	21.9	3.5	Thymic carcinoma	TC
25	67	M	5.7	21.0	8.9	Thymoma	MS

M-male, F-female, TC-transcervical, MS-median sternotomy, R -robotic resection, VATS-video assisted thoracic surgery

Author Manuscript

Author Manuscript

Author Manuscript

* subject underwent thoracosternotomy